JACS
JOURNAL OF THE AMERICAN CHEMICAL SOCIETY
Article
pubs.acs.org/JACS

Formation of Trivalent Zirconocene Complexes from *ansa*-Zirconocene-Based Olefin-Polymerization Precatalysts: An EPR- and NMR-Spectroscopic Study

Taylor N. Lenton,[†] John E. Bercaw,*[,†] Valentina N. Panchenko,[‡] Vladimir A. Zakharov,[‡] Dmitrii E. Babushkin,*[,‡] Igor E. Soshnikov,[‡] Evgenii P. Talsi,[‡] and Hans H. Brintzinger*[,§]

[†]Arnold and Mabel Beckman Laboratories of Chemical Synthesis, California Institute of Technology, Pasadena, California 91125, United States

[‡]Boreskov Institute of Catalysis, Russian Academy of Science, Siberian Branch, Pr. Lavrentieva 5, 630090 Novosibirsk, Russian Federation

[§]Fachbereich Chemie, Universität Konstanz, D-78457 Konstanz, Germany

Supporting Information

ABSTRACT: Reduction of Zr(IV) metallocenium cations with sodium amalgam (NaHg) produces EPR signals assignable to Zr(III) metallocene complexes. The chloro-bridged heterodinuclear *ansa*-zirconocenium cation $[(SBI)Zr(\mu\text{-}Cl)_2AlMe_2]^+$ (SBI = *rac*-dimethylsilylbis(1-indenyl)), present in toluene solution as its $B(C_6F_5)_4^-$ salt, thus gives rise to an EPR signal assignable to the complex $(SBI)Zr^{III}(\mu\text{-}Cl)_2AlMe_2$, while $(SBI)Zr^{III}$-Me and $(SBI)Zr^{III}(\mu\text{-}H)_2Al^iBu_2$ are formed by reduction of $[(SBI)Zr(\mu\text{-}Me)_2AlMe_2]^+$ $B(C_6F_5)_4^-$ and $[(SBI)Zr(\mu\text{-}H)_3(Al^iBu_2)_2]^+$ $B(C_6F_5)_4^-$, respectively. These products can also be accessed, along with $(SBI)Zr^{III}$-^{i}Bu and $[(SBI)Zr^{III}]^+$ AlR_4^-, when $(SBI)ZrMe_2$ is allowed to react with HAl^iBu_2, eliminating isobutane en route to the Zr(III) complex. Further studies concern interconversion reactions between these and other (SBI)Zr(III) complexes and reaction mechanisms involved in their formation.

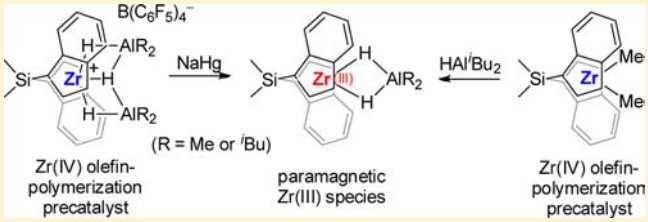

1. INTRODUCTION

Cationic, tetravalent group 4 metallocene complexes have been well established as active α-olefin polymerization catalysts.[1] Frequently, metallocene precatalysts are activated with methylaluminoxane (MAO), producing complex reaction mixtures,[2] in which metal species reduced by one electron to trivalent compounds can sometimes also be observed. *In situ* formation of Ti(III) species, which are apparently inactive, has been documented for titanocene-based polymerization catalysts.[3] While Ti(III) half-sandwich complexes have been reported to catalyze the polymerization of styrenes,[4] the role of various Ti oxidation states in these systems appears still controversial.[5]

Much less attention has been directed at the formation of Zr(III) species in the course of zirconocene-catalyzed olefin-polymerizations. Despite some clear EPR-spectroscopic evidence for the occurrence of Zr(III) species in zirconocene-based polymerization catalysts,[6,7] and substantial previous work on trivalent zirconocene complexes in general,[8] information about the nature and the reaction tendencies of Zr(III) complexes, which arise under polymerization conditions, is still rather limited. Identifying these reduced species and determining the mechanisms of their formation from Zr(IV) complexes present in active catalyst systems are first steps toward elucidating whether they exist as temporary resting states or are permanently removed from the catalytic cycle.

Additionally, we are interested in the role that aluminum hydrides play in polymerization systems,[9] as they are frequently introduced by loss of isobutene from triisobutylaluminum (TIBA), which is added to increase the overall activity of the catalytic system.[10] Previously it was shown that $[(SBI)Zr(\mu\text{-}Me)_2AlMe_2]^+$ (SBI = *rac*-dimethylsilylbis(1-indenyl)), a highly reactive intermediate in zirconocene-based polymerization catalysts,[11] is converted to $[(SBI)Zr(\mu\text{-}H)_3(Al^iBu_2)_2]^+$, itself a polymerization precatalyst,[12] when even small amounts of HAl^iBu_2 are present in solution.[13] Intriguingly, higher concentrations of paramagnetic compounds are observed by EPR spectroscopy upon activation with MAO/TIBA mixtures than with MAO alone, which might result from Zr(III) species being formed by the introduction of aluminum hydride compounds into these reaction systems.[7]

In light of the above information, we have sought to generate relevant zirconocene complexes of oxidation state Zr(III) by alternative routes, in order to provide spectral and reactivity data for comparison with zirconocene reaction systems during polymerization catalysis. In this report, we present results of NMR- and EPR-spectroscopic studies on reduction reactions of several (SBI)Zr(IV) complexes with sodium amalgam and with diisobutylaluminum hydride, which give access to a variety of

Received: March 29, 2013
Published: June 10, 2013

dx.doi.org/10.1021/ja403170u | J. Am. Chem. Soc. 2013, 135, 10710−10719

trivalent zirconocene species, and on interconversion reactions of some of these Zr(III) complexes. This should provide a more complete reference for studying Zr(III) products, that might arise under catalytic conditions, and offer first insights into possible mechanisms of their formation.

2. RESULTS AND DISCUSSION

Due to the complex nature of these reaction systems and the limited structural information that can be obtained by EPR spectroscopy alone, a combination of data is used here to identify and characterize Zr(III) species present in these reaction media. First, we consider the products that arise from the sodium amalgam reduction of various zirconocenium cations present under catalytic reaction conditions. Further studies concern the formation of Zr(III) compounds that might arise in catalytic systems upon interaction with dialkyl aluminum hydride compounds. Finally, we investigate the reactivity patterns of these species upon addition of aluminum chloride, aluminum alkyl and aluminum hydride compounds.

2.1. Reduction with Sodium Amalgam. While sodium amalgam (NaHg) has previously been a useful reductant for various metallocene complexes,[14−16] no change in the NMR spectra of C_6D_6 solutions of (SBI)$ZrMe_2$ (**1**) was observed upon shaking with NaHg, containing 1% (wt/wt) Na, for several hours. Prolonged stirring of a C_6D_6 solution of (SBI)$ZrCl_2$ (**2**) with NaHg for several days produced a color change to dark brown, but we were not able to isolate or identify any products from this reaction system. Several cationic zirconocenium complexes, on the other hand, proved to be more prone than these neutral species to give identifiable reduction products upon treatment with sodium amalgam.

A particularly straightforward reduction is observed from the dichloro-bridged cation $[(SBI)Zr(\mu\text{-}Cl)_2AlMe_2]^+$ (**3**), present in solution as its $B(C_6F_5)_4^-$ salt.[17] Reaction of NaHg with a toluene solution of **3** gives rise to an EPR spectrum with a signal at g = 1.958 (Figure 1). The shape of this signal, a midpoint inflection with reduced slope, indicates some unresolved hyperfine splitting. As in a similar case reported by Lyakin et al.,[7] a model spectrum calculated for interaction of the unpaired electron with one ^{27}Al and one ^{91}Zr nucleus is in near-perfect agreement with the observed spectrum and consistent with an assigned structure of (SBI)$Zr^{III}(\mu\text{-}Cl)_2AlMe_2$ (**4**). Crystallographic data which further confirm this assignment will be discussed in a later section, as **4** was generated using alternate methods to avoid the presence of (rather insoluble) $[Na][B(C_6F_5)_4]$ in the reaction system.

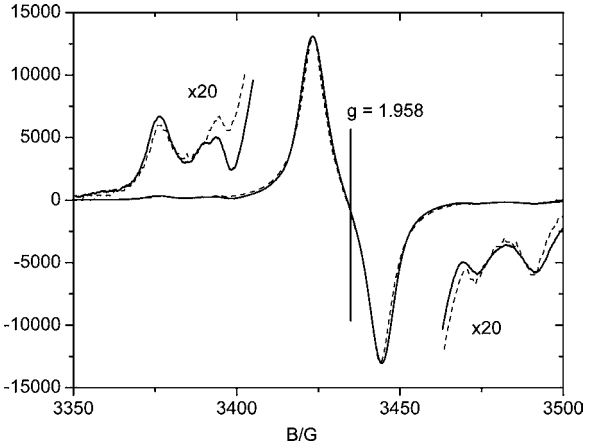

Figure 1. EPR spectrum (X-band, 25 °C) of **4**, the Zr^{III} complex obtained by NaHg-induced reduction of a 3.5 mM solution of $[(SBI)Zr(\mu\text{-}Cl)_2AlMe_2]^+$ $B(C_6F_5)_4^-$ in C_6D_6 (solid line), and EPR spectrum calculated for interaction of the unpaired electron with one ^{27}Al and one ^{91}Zr nucleus (100% ^{27}Al, I = 5/2, a(^{27}Al) = 3.4 G; 11% ^{91}Zr, I = 5/2, a(^{91}Zr) = 18.6 G, line width 5 G, dashed line).

The doubly integrated intensity of this signal accounts for, within accuracy limits, the total Zr content of the sample. In the absence of air, this signal is stable for days. Additionally, in ^1H NMR spectra of (SBI)$Zr^{III}(\mu\text{-}Cl)_2AlMe_2$, obtained by reduction of $[(SBI)Zr(\mu\text{-}Cl)_2AlMe_2]^+$ with the one-electron reductant cobaltocene,[16] two paramagnetically broadened signals with very short relaxation times of ∼4 ms appear, at 0.68 and −1.4 ppm, with intensities practically equal to those of the $(CH_3)_2Si$ and $Al(CH_3)_2$ signals seen for the initial cation $[(SBI)Zr(\mu\text{-}Cl)_2AlMe_2]^+$ before reduction (Supporting Information [SI]). These observations indicate that reaction of NaHg with the cation **3** furnishes the Zr(III) complex (SBI)$Zr^{III}(\mu\text{-}Cl)_2AlMe_2$ (**4**) according to eq 1 in practically quantitative yield.

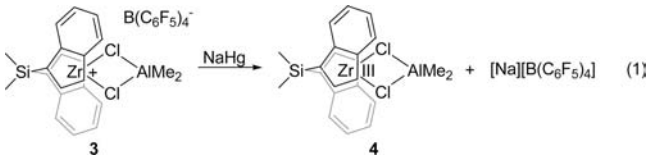

Quite a different course is taken by the $AlMe_3$-complexed methyl zirconocenium cation $[(SBI)Zr(\mu\text{-}Me)_2AlMe_2]^+$ (**5**), a prominent component of (SBI)Zr-based olefin-polymerization catalysts.[11] When a C_6D_6 solution of this heterobinuclear cation, prepared by reaction of 1 equiv of trityl tetrakis-(pentafluorophenyl)borate ($[Ph_3C][B(C_6F_5)_4]$) with **1** in the presence of $AlMe_3$, is shaken with sodium amalgam for ∼1 h, it produces the EPR spectrum shown in Figure 2.

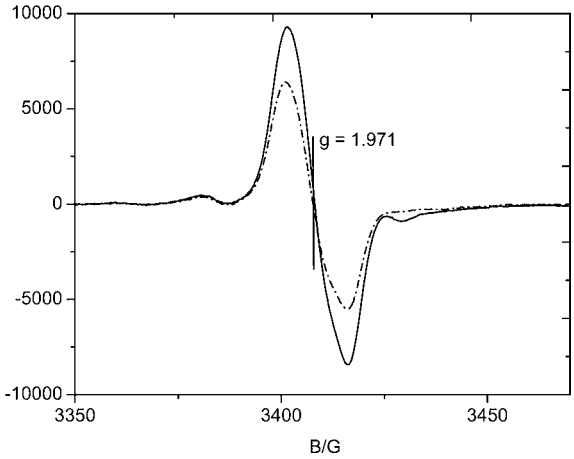

Figure 2. EPR spectrum (X-band, 25 °C) obtained after reduction of a 1 mM solution of $[(SBI)Zr(\mu\text{-}Me)_2AlMe_2]^+$ $B(C_6F_5)_4^-$ in C_6D_6 with 1% NaHg immediately (solid line) and ∼3 h after the end of the 1-h reaction period (broken line).

The EPR spectrum contains as its main component a signal centered at g = 1.971. On the basis of the absence of any ^{27}Al-associated hyperfine structure from the main signal in Figure 2, we can tentatively assume that this signal is due to the simple methyl complex (SBI)Zr^{III}-Me (**6**, eq 2),[19] rather than to the conceivable direct electron-uptake product (SBI)$Zr^{III}(\mu\text{-}Me)_2AlMe_2$.

dx.doi.org/10.1021/ja403170u | J. Am. Chem. Soc. 2013, 135, 10710−10719

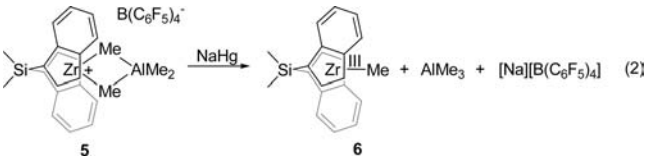

5 6

The signal shown in Figure 2 accounts, however, only for a rather small fraction (~10–20%) of the total zirconocene concentration. In order to elucidate the course of the reduction reaction in more detail, we followed the EPR and ^{1}H NMR spectra of the reaction mixture in parallel. The ^{1}H NMR signals of the cation $[(SBI)Zr(\mu\text{-}Me)_2AlMe_2]^+$ (**5**), initially the only signals discernible, completely disappear during the one-hour reduction period. At the same time, the appearance of the characteristic ^{1}H NMR signals of the dimethyl complex $(SBI)ZrMe_2$ (**1**) shows that this complex is formed in substantial concentration (about one-half of the initial concentration of the cation (**5**) during the reduction reaction (SI).[20] Reactions which might lead to the rather unexpected formation of **1** (itself not a reduction product) in the course of the reduction reaction will be discussed in a later section.

Finally, we have also studied the NaHg-induced reduction of the hydride-bridged cation $[(SBI)Zr(\mu\text{-}H)_3(AlR_2)_2]^+$ (**7**, R = Me or ^{i}Bu), another possible component of (SBI)Zr-based catalyst systems.[9] When a C_6D_6 solution of this cation, prepared by reaction of **1** with 1 equiv of $[Ph_3C][B(C_6F_5)_4]$ in the presence of 4 equiv of HAl^iBu_2,[13] is shaken for 1 h with sodium amalgam, it gives rise to the EPR spectrum shown in Figure 3. Apart from a minor, as yet not assignable component

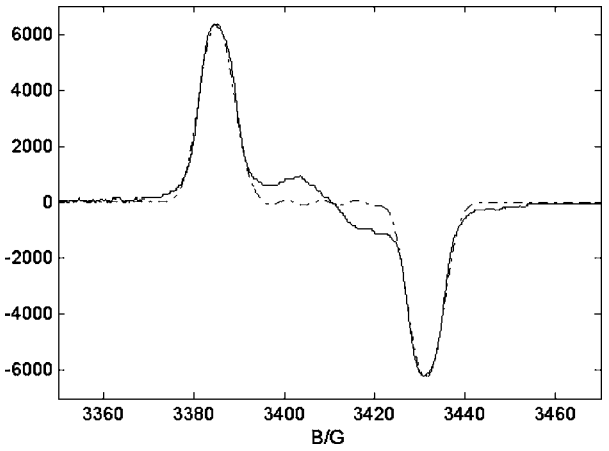

Figure 3. EPR spectrum (X-band, 25 °C) obtained from a 1 mM C_6D_6 solution of $[(SBI)Zr(\mu\text{-}H)_3(AlR_2)_2]^+$ after reduction with 1% NaHg (solid line) and EPR spectrum calculated for interaction of the unpaired electron with one ^{27}Al nucleus (100% ^{27}Al, $I = 5/2$, $a(^{27}Al) = 7.6$ G) and two ^{1}H nuclei (100% ^{1}H, $I = 1/2$, $a(^1H) = 4$ G, line width 7 G, broken line), assigned to $(SBI)Zr^{III}(\mu\text{-}H)_2AlR_2$ (**8**).

in its central part, the spectrum shows a main signal at $g = 1.970$. The shape of the main signal is indicative of a hyperfine splitting by a ^{27}Al nucleus, which is about twice as strong as that discussed above for the Cl-bridged species **4** (Figure 1).[21] Model spectra calculated with a hyperfine interaction constant of $a(^{27}Al) = 7.5$ G closely approach the main signal shown in Figure 3, provided that the hyperfine splitting in its central part is not resolved, either due to an unusually large line width of 10–12 G, or alternatively, by further unresolved hyperfine interaction with two ^{1}H nuclei, each with $a(^1H) \approx 4$ G and a more reasonable line width of 7–8 G (SI). We can thus tentatively assume that the main signal shown in Figure 3 is due to a dihydride-bridged complex $(SBI)Zr^{III}(\mu\text{-}H)_2AlR_2$ (**8** eq 3).[22,23] The intensity of the signal indicates that the yield of complex **8** is ~30%.

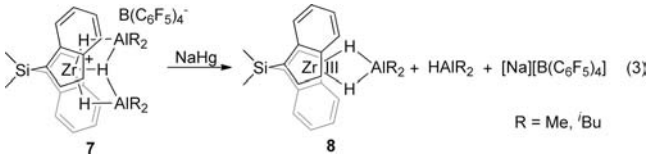

7 8

While the value of $a(^1H) \approx 4$ G in **8** might appear rather small for hydride ligands in direct contact with a Zr(III) center,[24–27] this assignment has precedence in the dihydride-bridged complex $(C_5H_5)_2Zr^{III}(\mu\text{-}H)_2Al(Me)(C_6H_2\text{-}2,4,6\text{-}^tBu)$, for which an EPR signal with $a(^{27}Al) = 8.7$ G and $a(^1H) = 3.9$ G has been reported by Wehmschulte and Power.[28] It must be taken into account that the $Zr^{III}(\mu\text{-}H)_2Al$ bonding situation differs distinctly from that of a terminal Zr^{III}-H unit. Since Al(III) is likely to have a higher electronegativity than Zr(III), the complex $(SBI)Zr^{III}(\mu\text{-}H)_2AlR_2$ is likely to display some character of an inner-sphere ion pair $(SBI)Zr^{III+}\cdots H_2AlR_2^-$. The diminished Zr–H covalency can thus be expected to result in reduced values of $a(^1H)$;[29] hence, a value of $a(^1H) \approx 4$ G would appear compatible with this assignment.

2.2. Reduction of $(SBI)ZrMe_2$ by HAl^iBu_2. While searching for causes for the incomplete progress of the reduction to **8**, described above, we noticed that EPR signals similar to that shown in Figure 3 are observed in solutions containing the dimethyl complex $(SBI)ZrMe_2$ (**1**) and HAl^iBu_2 even before the addition of $[Ph_3C][B(C_6F_5)_4]$ and/or NaHg. More detailed studies on this reaction are described below, along with subsequent reactivity studies aimed at further characterization.

A 3.5 mM solution of **1** in C_6D_6, which contains a 10-fold excess of HAl^iBu_2, slowly develops the EPR spectra shown in Figure 4. The spectrum obtained after about one day is practically identical to that produced by reduction of the cation $[(SBI)Zr(\mu\text{-}H)_3(AlR_2)_2]^+$ (**7**) with NaHg (Figure 3) and is assigned as the same hydride-bridged complex $(SBI)Zr^{III}(\mu\text{-}H)_2AlR_2$ (**8**). The intensity of this signal indicates that species **8**

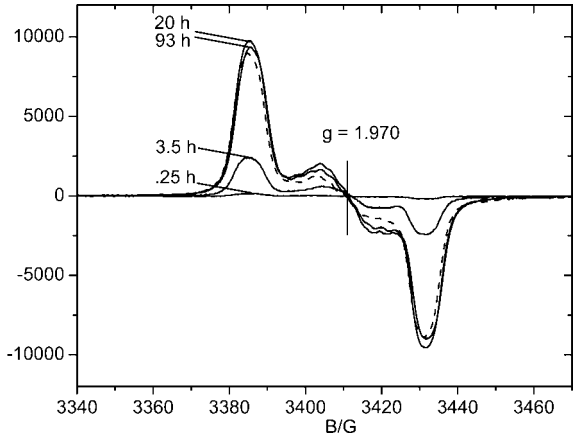

Figure 4. EPR spectrum (X-band, 25 °C) of a 3.5 mM solution of $(SBI)ZrMe_2$ in C_6D_6, which contains a 10-fold excess of HAl^iBu_2 at various reaction times (solid lines) and, for comparison, the spectrum assigned to **8**, taken from Figure 3 (broken line).

dx.doi.org/10.1021/ja403170u | J. Am. Chem. Soc. 2013, 135, 10710–10719

amounts to ~20% of the total Zr concentration at this time and does not grow any further at longer reaction times. Parallel ^{1}H NMR measurements reveal that the reaction is accompanied by formation of approximately one equiv of isobutane per unit of **1**,[30] together with traces of methane. Under these conditions, **8** thus appears to arise mainly by reductive elimination of isobutane (eq 4).

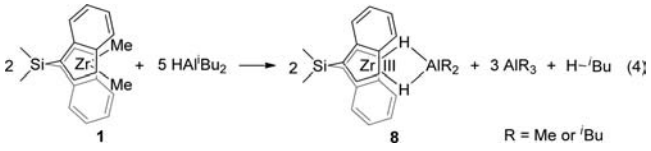

In a related experiment, a C_6D_6 solution of **1** containing only 2 equiv of HAl^{i}Bu$_2$, i.e. an amount less than that required by the stoichiometry of eq 4, developed the EPR spectra shown in Figure 5. The spectra still show the signal of **8** but are now

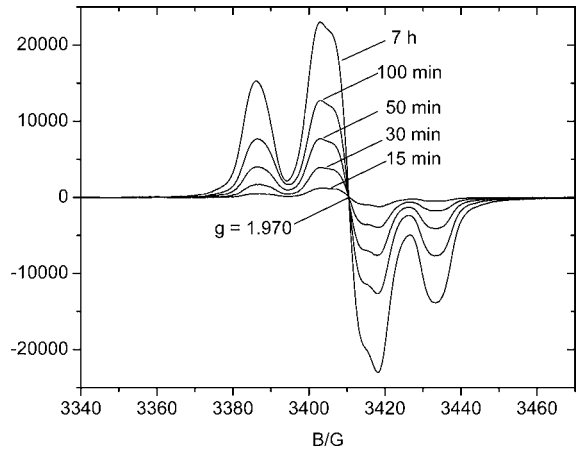

Figure 5. EPR spectra (X-band, 25 °C) of a 3.5 mM solution of (SBI)ZrMe$_2$ in C_6D_6, which contains 2 equiv of HAl^{i}Bu$_2$, at various reaction times.

dominated by a central signal, also at g = 1.970. This signal shows a partly resolved hyperfine splitting due to interaction of the unpaired electron with two ^{1}H nuclei, each with a(^{1}H) = 5.7 G (SI). On the basis of its g value, which is similar to that of the species (SBI)Zr^{III}-Me discussed above, and on the basis of its a(^{1}H) value, which is within the range of values previously reported for alkyl zirconocene complexes of oxidation stage Zr(III),[7,31] we assign this signal to the isobutyl complex (SBI)Zr^{III}-^{i}Bu (**9**). After a reaction period of several hours, **8** and **9** account together for about 90% of the total zirconocene concentration in this reaction mixture.

Parallel ^{1}H NMR measurements of the reaction mixture reveal that the appearance of the EPR signals shown in Figure 5 is accompanied again by substantial evolution of isobutane and methane—in this case in comparable amounts. Formation of isobutyl complex **9** by reductive alkane elimination can thus be described by eq 5

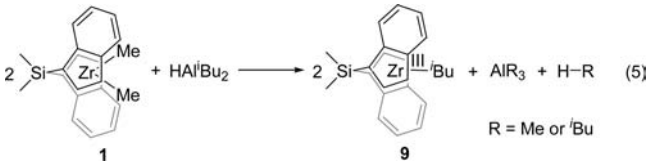

Formation of (SBI)Zr^{III}-^{i}Bu as the reduction product is further supported by the observation that addition of dimethylphenylphosphine to the product mixture generates, at the expense of the signals shown in Figure 5, a somewhat broadened EPR doublet with a hyperfine splitting of 10.6 G (SI), as would be expected for a phosphine complex of composition (SBI)Zr(^{i}Bu)PMe$_2$Ph, formed according to eq 6.[32]

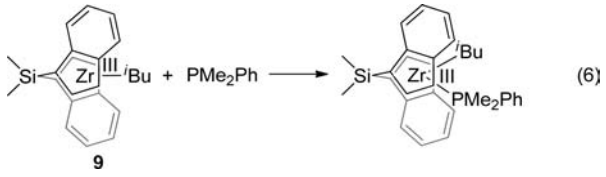

While we were not able to corroborate the structures of complexes **8** and **9** by crystal structure determinations, our assignment of the "outer-wings" signal shown in Figure 4 to (SBI)Zr^{III}(μ-H)$_2$Al^{i}Bu$_2$ (**8**) and of the central signal to (SBI)Zr^{III}-^{i}Bu (**9**) is supported by the following observation: Addition of HAl^{i}Bu$_2$ to a mixture of the two causes the signal assigned to **8** to increase relative to that of **9**, while the opposite is observed upon addition of Al^{i}Bu$_3$, i.e. an equilibrium reaction as in eq 7 appears to interconvert **8** and **9** (SI).

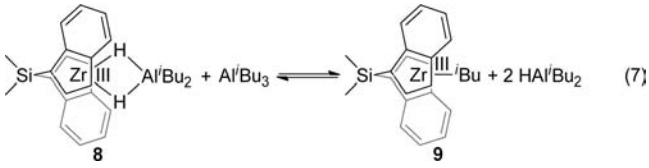

Formation of the dichloro-bridged complex **4** from **8** and **9** was studied by reacting a solution containing both of these species with increasing increments of ClAlMe$_2$. The EPR spectra obtained in this manner (Figure 6) clearly reveal a two-

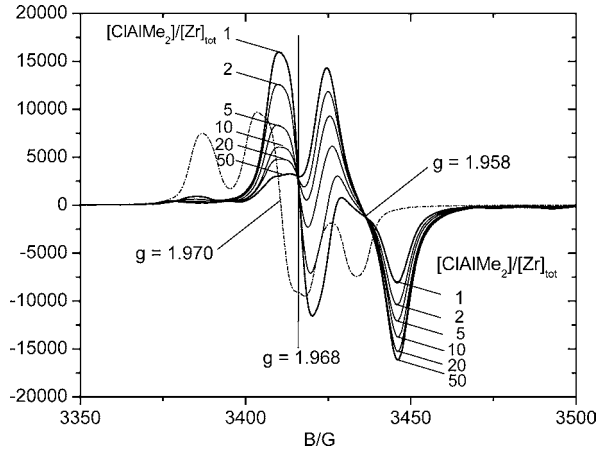

Figure 6. EPR spectra (X-band, 25 °C) of a 3.5 mM solution of (SBI)ZrMe$_2$ (**1**) in C_6D_6, which had reacted with 2 equiv of HAl^{i}Bu$_2$ for 16 h (broken line), after stepwise addition of 1–50 equiv of ClAl^{i}Bu$_2$ (solid lines, corrected for dilution).

step reaction: addition of only 1 equiv of ClAlMe$_2$ causes the practically complete conversion of all (SBI)Zr(III) species to a new complex with g = 1.968. Subsequent additions of ClAlMe$_2$ gradually convert this new complex to **4**. "Isosbestic" points at fields of 3416 and 3436 G indicate that only two (SBI)Zr(III) species are present under these conditions.

dx.doi.org/10.1021/ja403170u | J. Am. Chem. Soc. 2013, 135, 10710–10719

On the basis of these observations and the lack of obvious hyperfine interaction, the new signal at g = 1.968 might *prima facie* be assigned to the monochloro complex (SBI)Zr^{III}-Cl. Since this presumably Lewis-basic species would arise, however, in the presence of highly Lewis-acidic trialkyl aluminum compounds, it should most probably be designated as its AlR_3 adduct (SBI)Zr^{III}-$ClAlR_3$ (**10**). The presumably increased Zr···Al bond distance in this type of ion pair would diminish the resolution of any ^{27}Al hyperfine interaction beyond detection. This complex appears to be formed in practically quantitative yield under these conditions (eq 8), and is then converted to **4** by excess $ClAl^iBu_2$ in an equilibrium reaction (eq 9).

$$\underset{\mathbf{9}}{(SBI)Zr^{III}\text{-}{}^{i}Bu} + ClAlMe_2 \rightarrow \underset{\mathbf{10}}{(SBI)Zr^{III}\text{-}ClAlR_3} \quad (8)$$

$$\underset{\mathbf{10}}{(SBI)Zr^{III}\text{-}ClAlR_3} + ClAlMe_2 \rightleftharpoons \underset{\mathbf{4}}{(SBI)Zr^{III}(\mu\text{-}Cl)_2AlR_2} + AlR_3 \quad (9)$$

$R = Me, {}^{i}Bu$

In accord with eq 9, addition of excess $AlMe_3$ to a solution of species **4** decreases its EPR signal at g = 1.958 with concomitant appearance of the signal of Al-stabilized Cl species **10** at g = 1.968 (SI). The observation that excess trialkyl aluminum causes conversion of **4** to the monochloride complex supports our tentative proposal that the latter is present in form of a trialkyl aluminum adduct.

Addition of increasing proportions of HAl^iBu_2, on the other hand, to a solution containing **4** converts most of the latter to **8**, but superimposed on the signal of this species at g = 1.970 remains the signal of **10** at g = 1.968 (SI). While the equilibrium represented in eq 10 thus appears to be movable to either side, the Cl ligand in (SBI)Zr^{III}-$ClAlR_3$ obviously resists exchange with an Al-bound ^{i}Bu group.

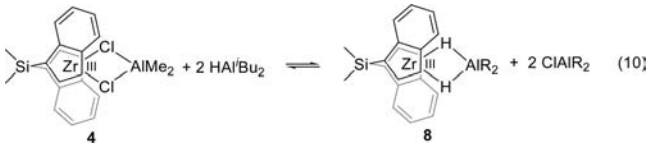

2.3. Crystal and Molecular Structure of (SBI)Zr^{III}(μ-Cl)$_2$$AlR_2$ (4). Taking advantage of these equilibria (eqs 9 and 10), **4** can be obtained as a solution in pentane by first allowing **1** to react overnight with 2 equiv of HAl^iBu_2 and then treating the resulting mixture of **8** and **9** with excess $ClAlMe_2$. When such a solution was cooled slowly to −20 °C, it produced crystals of X-ray quality (SI). Structure determination of these crystals revealed a $P2/c$ space group and a unit cell with β = 92.126(2)° and four molecules of **4** with both enantiomers in equal proportions (Figure 7). The final anisotropic full-matrix least-squares refinement on F^2 yielded a molecular structure for **4** in agreement with the spectral data discussed above (Figure 7).

The coordination geometry of the Zr center of **4** can be compared to that of $(SBI)ZrCl_2$ (**2**),[33] as well as to those of several other zirconocene chloride complexes of oxidation state Zr(III), *viz.* $[(Me_3Si\text{-}C_5H_4)_2Zr^{III}(\mu\text{-}Cl)]_2$,[34] $[(1,3\text{-}(Me_3Si)_2\text{-}C_5H_3)_2Zr^{III}(\mu\text{-}Cl)]_2$,[35] and $[(C_5H_5)Zr^{III}(\mu\text{-}Cl)]_2\text{-}\mu\text{-}(C_5H_4\text{-}C_5H_4)$[36] (Table 1). The distance of the C_5-ring centroid from the Zr center is found—somewhat unexpectedly—to be smaller by ∼0.1 Å for the Zr(III) complex **4** than for its Zr(IV) congener **2**. This observation and the substantially longer Zr−Cl distances in **4** than in **2** conform with the notion that the extra electron resides in a molecular orbital of **4** which is antibonding with regard to the Cl ligands but mainly nonbonding with respect to the ring ligands.[37]

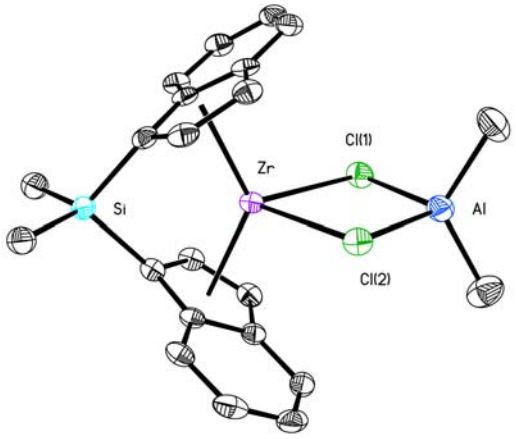

Figure 7. Molecular structure of (SBI)Zr^{III}(μ-Cl)$_2$$Al(CH_3)_2$ (**4**) with thermal ellipsoids at the 50% probability level. H atoms omitted for clarity. For selected bond lengths and angles see Table 1.

Additionally, Zr^{III}-Cl distances are found to be significantly longer for **4** than for the dimeric Zr(III) chloride compounds listed in Table 1. The Al−Cl distances, on the other hand are shorter in **4** than those reported for a number of dimeric $[R_2Al(\mu\text{-}Cl)]_2$ compounds (2.32−2.35 Å) and close to those in the electron-poor perfluorinated compound $[(C_6F_5)_2AlCl]_2$ (Table 2).[38−41] These deviations of Zr−Cl and Al−Cl bond distances in the heterobinuclear species **4** from values reported for related homobinuclear species—as well as its conspicuously diminished Cl−Zr−Cl and widened Cl−Al−Cl angles—can all be considered to suggest that (SBI)Zr^{III}(μ-Cl)$_2$$Al(CH_3)_2$ is indeed approaching the bonding situation of a contact ion pair $(SBI)Zr^{III+}\cdots Cl_2Al(CH_3)_2^-$.

Attempts to crystallize in a similar manner also other (SBI)Zr(III) complexes, in particular complexes **8** and **9**, were not successful, most likely due to the lower polarity of these compounds.

2.4. Formation of a Cationic Zirconium(III) complex. The Zr(III) compounds discussed above seem to be relatively stable, but isobutyl compound **9** undergoes a slow, further transformation to give a signal centered at g = 1.983. When the reaction between **1** and 2 equiv of HAl^iBu_2 (Figure 5), is observed for longer reaction times, it yields the spectral changes shown in Figure 8. Over the course of several days, the signals of **8** and **9** both diminish to ∼10% of their previous size, while a new signal grows which is centered at g = 1.983. After about one week, little if any further changes occur. Some loss of overall signal intensity appears to occur over this period of time.

Spectral changes of the same kind occur to a more complete extent if a 3.5 mM solution of **1** is allowed to react with only 1 equiv of HAl^iBu_2. In this case, we observe, after ∼6 days, only the signal centered at g = 1.983 (Figure 9).[42] This rather narrow signal shows a hyperfine splitting due to the ^{91}Zr nucleus with $a(^{91}Zr)$ = 17 G, but no signs of other hyperfine interactions.

Signals with similar g-values and hyperfine splitting, previously observed after reduction of $(C_5H_5)_2ZrCl_2$ with BuLi and in MAO-activated toluene solutions of (2-Ph-

dx.doi.org/10.1021/ja403170u | J. Am. Chem. Soc. 2013, 135, 10710−10719

Table 1. Selected Bond Lengths (Å) and Angles (deg) for a Series of Zirconocene Compounds

	Zr−Cl	Cl−Zr−Cl	Zr−CT	CT−Zr−CT	ref
(SBI)$Zr^{III}(\mu\text{-}Cl)_2AlMe_2$ (**4**)	2.650(1) 2.624(1)	77.07(3)	2.1908 2.1836	130.70	this work
(SBI)$ZrCl_2$ (**2**)	2.431(<1)	98.76(1)	2.293	119.04	33
$[(Me_3Si\text{-}C_5H_4)_2Zr^{III}(\mu\text{-}Cl)]_2$	2.560 ± 4[a]	93.34 ± 0.10[b]			34
$[(1,3\text{-}(Me_3Si)_2\text{-}C_5H_3)_2Zr^{III}(\mu\text{-}Cl)]_2$	2.602 ± 6[a]	82.77 ± 1.10[b]			35
$[(C_5H_5)Zr^{III}(\mu\text{-}Cl)]_2\text{-}(\mu\text{-}C_5H_4{-}C_5H_4)$	2.578	100			36

[a]Averages of multiple Zr−Cl bond lengths. [b]Averages of multiple Cl−Zr−Cl bond angles.

Table 2. Selected Bond Lengths (Å) and Angles (deg) for a Series of Aluminum Compounds

	Al−Cl	Cl−Al−Cl	Al−R	ref
(SBI)$Zr(\mu\text{-}Cl)_2AlMe_2$ (**4**)	2.253(1) 2.263(1)	93.37(5)	1.941(4) 1.946(4)	this work
$[^tBu_2Al(\mu\text{-}Cl)]_2$	2.316(3) 2.324(3)	87.2(1)	1.966(6) 1.982(9)	38
$[Mes_2Al(\mu\text{-}Cl)]_2$	2.346(2) 2.315(2)	85.2(1)	1.972(4) 1.966(5)	39
$[AlMe(CSiR_3)(\mu\text{-}Cl)]_2$	2.3216(12)	86.53(4)	1.938(4)	40
$[(C_6F_5)_2AlCl]_2$	2.244(1) 2.273(1)	90.60 90.75	1.953(3) 1.944(3)	41

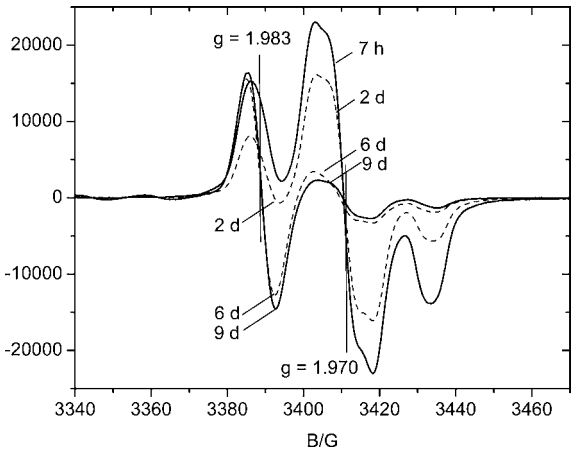

Figure 8. EPR spectra (X-band, 25 °C) of a 3.5 mM solution of (SBI)$ZrMe_2$ in C_6D_6, which contains 2 equiv of HAl^iBu_2 (cf. Figure 5), measured after increasing reaction times.

ind)$_2ZrCl_2$ and (SBI)$ZrCl_2$, were assigned to the cations $[Cp_2Zr^{III}]^+$, $[(2\text{-Ph-ind})_2Zr^{III}]^+$, and $[(SBI)Zr^{III}]^+$, respectively, on the basis of their lack of ligand hyperfine structure and their low-field position.[7,43] We follow this proposal in tentatively assigning the signal at g = 1.983, shown in Figure 7, to the "free" cation $[(SBI)Zr^{III}]^+$ (**11**, eq 11) .

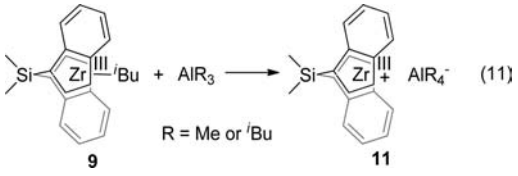

This assignment raises the question of how such a cationic species could arise in a reaction system free of any of the typical cationization reagents, such as MAO or trityl cation, and which kind of anion would be associated with it. Inspection of eq 11 suggests that the "spontaneous ionization" represented there is likely to be exergonic, since an aluminum trialkyl is most likely a stronger Lewis acid than the $[(SBI)Zr^{III}]^+$ cation and thus prone to abstract an $^iBu^-$ ligand from the latter. The resulting ion pair $[(SBI)Zr^{III}]^+$ AlR_4^- would then differ from inner-sphere ion pairs such as $(SBI)Zr^{III+}\cdots Cl_2AlR_2^-$ and (SBI)-$Zr^{III+}\cdots H_2AlR_2^-$, discussed above as representations of the chloride- and hydride-bridged complexes **4** and **8**. Apparently, the alkyl periphery of an anion AlR_4^- has a much lower tendency to coordinate to a Zr(III) center than the chloride or hydride units of a $Cl_2AlR_2^-$ or an $H_2AlR_2^-$ anion, such that the cation $[(SBI)Zr^{III}]^+$ associates with the anion AlR_4^- predominantly in an outer-sphere ion pair.

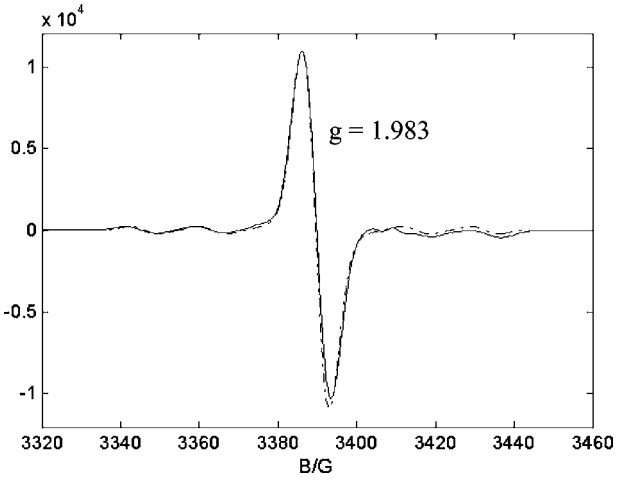

Figure 9. EPR spectrum (X-band, 25 °C) of **11**, generated from a 3.5 mM solution of **1** in C_6D_6, which contains 1 equiv of HAl^iBu_2, after a reaction time of ~6 days (solid line) and spectrum calculated for a hyperfine splitting due to a ^{91}Zr nucleus (11% ^{91}Zr, I = 5/2, a(^{91}Zr) = 17 G).

Consistent with this proposal is the observation that addition of HAl^iBu_2 (50 equiv) to a solution containing the ion pair **11** causes the signal at g = 1.983 to disappear, while regenerating the signal pattern of the dihydride-bridged complex **8** (SI). Apparently, scrambling of alkyl and hydride units between neutral and anionic aluminum alkyls leads to formation of $H_2Al^iBu_2^-$, which upon association with $[(SBI)Zr^{III}]^+$ gives $(SBI)Zr^{III+}\cdots H_2AlR_2^- \equiv (SBI)Zr^{III}(\mu\text{-}H)_2AlR_2$.

This notion would also provide an explanation for the rather unexpected formation of (SBI)$ZrMe_2$ (**1**)—itself not a reduction product—in the course of the NaHg-induced reduction of the dimethyl-bridged cation **5**, noted in section 2.1, Reduction with Sodium Amalgam. Formation of **1** is not explicable by a disproportionation of $(SBI)Zr^{III}$-Me (**6**), one of the reduction products, to **1** and some (SBI)Zr complex of oxidation stage Zr(II), since **6** is found to be quite stable when prepared, in analogy to the reaction in eq 4, by reaction of **1**

dx.doi.org/10.1021/ja403170u | J. Am. Chem. Soc. 2013, 135, 10710−10719

with 5−10 equiv of $HAlMe_2$ (instead of HAl^iBu_2) followed by excess $AlMe_3$ (SI).

If, however, the cation $[(SBI)Zr^{III}(\mu\text{-}Me)_2AlMe_2]^+$ (**5**) would be initially reduced directly to $(SBI)Zr^{III}(\mu\text{-}Me)_2AlMe_2$, this species with its unfavorable alkyl bridges might arise only as a short-lived intermediate and rapidly dissociate to $[(SBI)Zr^{III}]^+$ and $AlMe_4^-$ (eq 12). The rather basic anion $AlMe_4^-$ would then most likely react with the highly Lewis-acidic Zr(IV) cation **5** so as to release **1** (eq 13). This reaction sequence would generate, in accord with our experimental results (SI, Figure S1) 0.5 equiv of **1** for each cation $[(SBI)Zr(\mu\text{-}Me)_2AlMe_2]^+$ reduced, while the coordinatively unsaturated cation **11** could react further with NaHg to yield some yet unidentified zirconocene species of oxidation state Zr(II).

$$\underset{\mathbf{5}}{[(SBI)Zr(\mu\text{-}Me)_2AlMe_2]^+} + NaHg \rightarrow \underset{\mathbf{11}}{[(SBI)Zr^{III}]^+} + [AlMe_4]^- + Na^+ \quad (12)$$

$$\underset{\mathbf{5}}{[(SBI)Zr(\mu\text{-}Me)_2AlMe_2]^+} + [AlMe_4]^- \rightarrow \underset{\mathbf{1}}{(SBI)ZrMe_2} + 2AlMe_3 \quad (13)$$

2.5. Mechanisms of Zr(III) Formation. The dihydride-bridged complex $(SBI)Zr^{III}(\mu\text{-}H)_2AlR_2$ (**8**) and the isobutyl complex $(SBI)Zr^{III}\text{-}^iBu$ (**9**) are formed, according to eqs 4 and 5, when $(SBI)ZrMe_2$ (**1**) is treated with varying amounts of HAl^iBu_2. Under these conditions, the Zr(III) products thus appear to arise mainly by reductive elimination of the alkanes isobutane and methane. Conceivable mechanisms for a reduction of Zr(IV) to Zr(III) centers by alkane elimination might be gleaned from the following observations: Immediately upon addition of HAl^iBu_2 to solutions of **1**, the HAl and ZrMe ^1H NMR signals of the reagents disappear and are replaced by broad signals, the intensities and positions of which depend on the $[HAl^iBu_2]_{init}/[Zr]_{tot}$ ratios used (SI). These changes indicate the formation of H/Me exchange products and/or adducts between HAl^iBu_2 and **1**. While our data do not allow an unequivocal identification of these intermediary reaction products, we assume that they are analogs, with Me in place of Cl, of those formed from $(SBI)ZrCl_2$ and HAl^iBu_2,[9c] i.e. heterobinuclear dihydride-bridged Zr(IV) species of the type shown in eq 14.

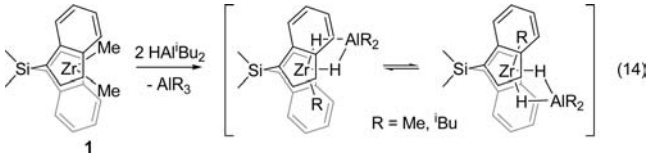

(14)

While these species would fulfill the formal requirement for reductive alkane elimination, viz. cis-positioned hydride and alkyl ligands, alternative and possibly more facile reaction paths might start from homodinuclear complexes which should be accessible from these heterobinuclear species *via* equilibria of the type represented in eq 15.

Rather than leading to Zr(II) products, which would arise by alkane elimination from heterobinuclear Zr(IV) species of the type shown in eq 14, alkane elimination from homobinuclear species, as in eq 15, would lead directly to Zr(III) reduction products (eq 16), which could then yield the final products,

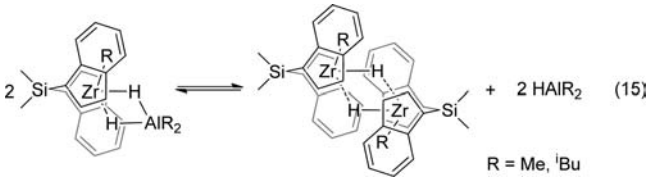

(15)

$(SBI)Zr^{III}(\mu\text{-}H)_2AlR_2$ and $(SBI)Zr^{III}\text{-}^iBu$, by subsequent association or ligand exchange with HAl^iBu_2.

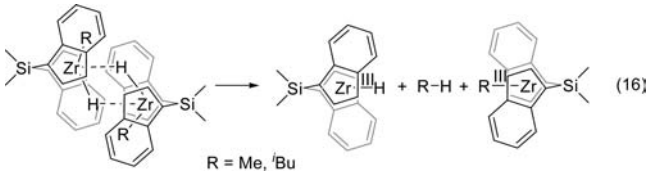

(16)

Our proposal, that homobinuclear complexes might be involved in the reduction process, is supported by the following observation: At a ratio of $[HAl^iBu_2]_{init}/[Zr]_{tot} = 2$, formation of Zr(III) products from $(SBI)ZrMe_2$ and HAl^iBu_2 occurs with a half-life of about 1.5 h. The half-life of this reaction increases unexpectedly to ∼5.5 h when (under otherwise identical conditions) HAl^iBu_2 is used at a higher ratio of $[HAl^iBu_2]_{init}/[Zr]_{tot} = 10$. This counterintuitive observation would be explained by the involvement of HAl^iBu_2 in the equilibrium represented in eq 15: An excess of HAl^iBu_2 would favor formation of heterobinuclear species at the expense of homobinuclear complexes and would thus be expected to decrease the rate of Zr(III) formation, if homobinuclear complexes are indeed required for efficient reductive alkane elimination.

3. CONCLUSIONS

On the basis of the evidence described above, six (SBI)Zr(III) species appear to be accessible by reduction processes starting from $(SBI)ZrMe_2$ (**1**) in the presence of Lewis-acidic organoaluminum compounds. These are two complexes with η^2-bound aluminate ligands, $(SBI)Zr^{III}(\mu\text{-}Cl)_2AlR_2$ (**4**) and $(SBI)Zr^{III}(\mu\text{-}H)_2AlR_2$ (**8**), three complexes with simple η^1-bound ligands, $(SBI)Zr^{III}\text{-}Me$ (**6**), $(SBI)Zr^{III}\text{-}^iBu$ (**9**), and $(SBI)Zr^{III}\text{-}ClAlR_3$ (**10**), and the cation $[(SBI)Zr^{III}]^+$ (**11**). Our EPR results indicate that these species are connected to one another and/or to $(SBI)ZrMe_2$ (**1**), by the reactions summarily represented in Scheme 1.

Most of these complexes appear to be coordinatively unsaturated, with valence-electron counts of 13 for $[(SBI)Zr^{III}]^+$ and 15 for $SBZr^{III}\text{-}X$ (with X = $ClAlR_3$, Me or ^{i}Bu). Even for $(SBI)Zr^{III}(\mu\text{-}X)_2AlR_2$, (with X = H or Cl), the effective electron density at the metal center is probably lower than suggested by their formal 17-electron count, due to the polar character of their Zr-ligand bonding, which might be written as $(SBI)Zr^{III+}\cdots X_2AlR_2^-$ (with X = H or Cl). The trivalent entities encountered in this study appear to have metal centers of lower electronegativity than the Zr(IV) centers of their tetravalent precursors, and hence an increased tendency to transfer their ligands to Lewis-acidic aluminum compounds present in the reaction medium.

In the course of these studies, we have not been able to obtain any clear indication of stable homobinuclear dimers of the type $(SBI)Zr^{III}(\mu\text{-}X)_2Zr^{III}(SBI)$, with X = Cl, H, or alkyl. Monomeric and dimeric forms of trivalent zirconocene chlorides have both been reported with complexes $[(Me_3Si\text{-}$

dx.doi.org/10.1021/ja403170u | J. Am. Chem. Soc. 2013, 135, 10710−10719

Scheme 1

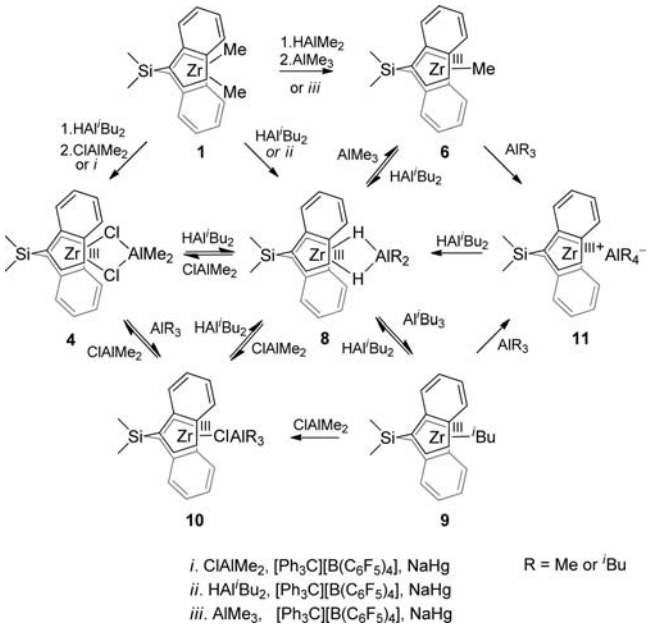

$C_5H_4)_2Zr^{III}(\mu\text{-Cl})]_2$,[34] and $[(1,3\text{-}(Me_3Si)_2\text{-}C_5H_3)_2Zr^{III}(\mu\text{-Cl})]_2$,[35] existing as dimers in the solid state, whereas $(1,3\text{-}(Me_3C)_2\text{-}C_5H_3)_2Zr^{III}Cl$, with doubly Me_3C-substituted rings, is monomeric.[44] The propensity of a trivalent zirconocene chloride to associate to a Cl-bridged dimer thus appears to be determined by rather subtle changes in the steric load of its ring ligands. While we cannot assess how a "free" $(SBI)Zr^{III}Cl$ species would range in this regard, its monomeric form is apparently stabilized by formation of the AlR_3 adduct, $(SBI)Zr^{III}ClAlR_3$ (**10**).

Similar considerations are likely to apply also to $(SBI)Zr^{III}$-hydride species, where adduct formation with a dialkylaluminum hydride is evident from the EPR spectra of **8**. For $(SBI)Zr^{III}$-alkyl species, on the other hand, no tendency to form any stable alkyl-bridged heterodinuclear adducts with alkylaluminum compounds is apparent from our data. Here, we can assume that a similarly low propensity of alkyl ligands to occupy a bridging position would also thwart any tendency of $(SBI)Zr^{III}$-alkyl species to form alkyl-bridged dimers.

At any rate, the EPR signal of $(SBI)Zr^{III}(\mu\text{-Cl})AlR_3$ (**10**) at g = 1.968 accounts for practically the entire zirconocene concentration, as does that of $(SBI)Zr^{III}(\mu\text{-Cl})_2AlMe_2$ (**4**), with which it is in equilibrium according to eq 9 (cf. Figure 8), and the Zr(III) complexes **8** and **9**, produced by reaction of **1** with 2 equiv of HAl^iBu_2. Any EPR-silent dimers of the type $[(SBI)Zr^{III}(\mu\text{-X})]_2$, with X = Cl, H, or alkyl, could thus represent only insignificant fractions of the zirconocene concentration in these reaction systems.

For some reaction systems, however, such as those where **1** reacts with 10 equiv of HAl^iBu_2, the resulting EPR signals account only for rather small fractions (20−30%) of the total zirconocene content. In these, as in some of the other reaction systems, the appearance of new ^1H NMR signals indicates the formation of some diamagnetic products, which we have not been able to identify so far. To which degree, for example, products of the (SBI)Zr(II) oxidation stage accumulate in the course of these reactions must thus remain open.

In our present study we have obtained first evidence concerning some relevant structures and reaction patterns of trivalent *ansa*-zirconocene complexes occurring in catalysis-related reaction media. Further studies will be aimed at elucidating the role these Zr(III) species play in zirconocene-based olefin-polymerization catalysis and if, once formed under polymerization conditions, they exist permanently in this oxidation state or can react further to regenerate Zr(IV) precatalysts.[45]

4. EXPERIMENTAL SECTION

All operations were carried out under a protective dinitrogen atmosphere, either in a glovebox or on a vacuum manifold. Solvents (benzene, toluene, benzene-d_6, toluene-d_8) were degassed and dried over 3-Å molecular sieves for 12 h or filtered through a plug of activated alumina. $(SBI)ZrMe_2$ was obtained from Dr. M. Ringwald, MCAT, Konstanz. Trimethylaluminum, diisobutylaluminum hydride, aluminum chloride, triisobutylaluminum (1 M in toluene), and dimethylphenylphosphine were used as obtained from Aldrich Chemical Co., Milwaukee. Dimethylaluminum hydride was synthesized as previously reported.[13] Stock solutions of diisobutylaluminum hydride, dimethylphenylphosphine, and dimethylaluminum chloride were made at two concentrations (280 mM and 28 mM) in toluene and benzene-d_6.

Solutions of $[(SBI)Zr(\mu\text{-Cl})_2AlMe_2][B(C_6F_5)_4]$,[13,17] $[(SBI)Zr(\mu\text{-H})_3(Al^iBu_2)_2][B(C_6F_5)_4]$,[13] and $[(SBI)Zr(\mu\text{-Me})_2AlMe_2][B(C_6F_5)_4]$[11] were prepared in analogy to previous reports.

Samples for NMR and EPR spectra were prepared in the glovebox by transferring 0.8 mL of prepared sample solutions into 5-mm OD glass NMR tubes. These were closed with rubber stoppers which had been washed with pentane and dried extensively *in vacuo*. For each measurement, these sample tubes were taken from the glovebox to the respective spectrometer and immediately transferred back to the glovebox for storage.

EPR spectra were measured using a Magnettech Miniscope MS400 spectrometer at an X-band frequency of 9.41 GHz. Hyperfine interaction parameters and g values were analyzed by model calculations using the software EASYSPIN.[46] Concentration of Zr(III) species were obtained by double integration of the EPR signal, compared to reference samples of TEMPO. NMR spectra were measured using Varian Inova 500, 600, or Mercury 300 spectrometers. Chemical shifts are referenced to residual solvents' peaks, 7.16 ppm for benzene and 2.08 ppm for CD_2H proton resonances of toluene. Further experimental details are described in the Supporting Information.

CAUTION: alkylaluminum compounds are pyrophoric and must be handled with special precautions (see, e.g., Shriver, D. F. *The Manipulation of Air-sensitive Compounds*; Robert E. Krieger Publishing Company: Malabar, FL, 1982).

■ ASSOCIATED CONTENT

Ⓢ Supporting Information

Further ^1H NMR and EPR data, simulations of EPR spectra, experimental details, and crystallographic information file. This material is available free of charge via the Internet at http://pubs.acs.org.

■ AUTHOR INFORMATION

Corresponding Author

Bercaw@caltech.edu (J.E.B.); Dimi@catalysis.ru (D.E.B.); hans.brintzinger@uni-konstanz.de (H.H.B.).

Notes

The authors declare no competing financial interest.

Crystallographic data for crystals containing the compound $(SBI)Zr(\mu\text{-Cl})_2AlMe_2$ (TNL17) have been deposited with the CCDC, 12 Union Road, Cambridge CB2 1EZ, UK; copies can be obtained on request, free of charge, by quoting the publication reference and deposition number 941568.

■ ACKNOWLEDGMENTS

This research was supported by Deutsche Forschhungsgemeinschaft (Grant Me1388/9-1), by the Russian Foundation of Basic Research (Grant 10-03-91330) and by US DOE, Office of Basic Energy Sciences (Grant DE-FG03-85ER13431). We thank Prof. Jay A. Labinger (California Institute of Technology), Dr. Konstantin P. Bryliakov (Boreskov Institute of Catalysis,) and Prof. Heiko Möller (University of Konstanz) for helpful discussions; Anke Friemel, Evelyn Wuttke, Martin Spitzbarth (University of Konstanz), David VanderVelde, and Angelo DiBilio (California Institute of Technology) for help with the acquisition and analysis of NMR and EPR spectra; and Lawrence M. Henling and Thomas S. Teets for assistance with mounting crystals and solving cyrstal structures. The Bruker KAPPA APEXII X-ray diffractometer was purchased via an NSF CRIF:MU award to the California Institute of Technology (CHE-0639094).

■ REFERENCES

(1) Reviews: (a) Resconi, L.; Cavallo, L.; Fait, A.; Piemontesi, F. *Chem. Rev.* **2000**, *100*, 1253−1345. (b) Resconi, L.; Chadwick, J. C.; Cavallo, L. In *Comprehensive Organometallic Chemistry III*; Crabtree, R. H., Mingos, D. M. P., Eds.; Elsevier: Oxford, 2007; Vol. *4*, Bochmann, M., Vol. Ed.; Chapter 4.09, pp 1005−1166.

(2) Reviews: (a) Chen, E. Y. X.; Marks, T. J. *Chem. Rev.* **2000**, *100*, 1391−1434. (b) Bochmann, M. *J. Organomet. Chem.* **2004**, *689*, 3982−3998. (c) Bochmann, M. *Organometallics* **2010**, *29*, 4711−4740.

(3) (a) Huang, Y. H.; Yu, Q.; Zhu, S.; Rempel, G. L.; Li, L. *J. Polym. Sci., Part A: Polym. Chem.* **1999**, *37*, 1465−1472. (b) Bryliakov, K. P.; Babushkin, D. E.; Talsi, E. P.; Voskoboynikov, A. Z.; Gritzo, H.; Schröder, L.; Damrau, H.-R. H.; Wieser, U.; Schaper, F.; Brintzinger, H. H. *Organometallics* **2005**, *24*, 894−904.

(4) (a) Grassi, A.; Saccheo, S.; Zambelli, A.; Laschi, F. *Macromolecules* **1998**, *31*, 5588−5591. (b) Chien, J. W. C.; Salajka, Z.; Dong, S. *Macromolecules* **1992**, *25*, 3199. (c) Mahanthappa, M. K.; Waymouth, R. M. *J. Am. Chem. Soc.* **2001**, *123*, 12093−12094.

(5) (a) Williams, E. F.; Murray, M. C.; Baird, M. C. *Macromolecules* **2000**, *33*, 261−268. (b) Bryliakov, K. P.; Semikolenova, N. V.; Zakharov, V. A.; Talsi, E. P. *J. Organomet. Chem.* **2003**, *683*, 23−28. (c) Napoli, M.; Grisi, F.; Longo, P. *Macromolecules* **2009**, *42*, 2516−2522.

(6) Cram, D.; Sartori, F.; Maldotti, A. *Macromol. Chem. Phys.* **1994**, *195*, 2817−2826.

(7) Lyakin, O. Y.; Bryliakov, K. P.; Panchenko, V. N.; Semikolenova, N. V.; Zakharov, V. A.; Talsi, E. P. *Macromol. Chem. Phys.* **2007**, *208*, 1168−1175.

(8) Review: Lancaster, S. J. In *Comprehensive Organometallic Chemistry III*; Crabtree, R. H., Mingos, D. M. P., Eds.; Elsevier, Oxford, 2007, Vol. *4*, Bochmann, M., Vol. Ed.; Chapter 4.07, p 741−757.

(9) (a) Babushkin, D. E.; Brintzinger, H. H. *Chem.—Eur. J.* **2007**, *13*, 5294−5299. (b) Babushkin, D. E.; Panchenko, V. N.; Timofeeva, M. N.; Zakharov, V. A.; Brintzinger, H. H. *Macromol. Chem. Phys.* **2008**, *209*, 1210−1219. (c) Baldwin, S. M.; Bercaw, J. E.; Brintzinger, H. H. *J. Am. Chem. Soc.* **2008**, *130*, 17423−17433.

(10) Kleinschmidt, R.; van der Leek, Y.; Reffke, M.; Fink, G. *J. Mol. Catal. A: Chem.* **1999**, *148*, 29−41.

(11) Bochmann, M.; Lancaster, S. J. *Angew. Chem., Int. Ed. Engl.* **1994**, *33*, 1634−1637.

(12) Baldwin, S. M.; Bercaw, J. E.; Brintzinger, H. H. *J. Am. Chem. Soc.* **2010**, *132*, 13969−13971.

(13) Baldwin, S. M.; Bercaw, J. E.; Henling, L. M.; Day, M. W.; Brintzinger, H. H. *J. Am. Chem. Soc.* **2011**, *133*, 1805−1813.

(14) Wailes, P. C.; Weigold, H. *J. Organomet. Chem.* **1971**, *28*, 91−95.

(15) Cuenca, T.; Royo, P. *J. Organomet. Chem.* **1985**, *293*, 61−67.

(16) Review: Connelly, N. G.; Geiger, W. E. *Chem. Rev.* **1996**, *96*, 877−910.

(17) Formation of the dichloro-bridged cation $[(SBI)Zr(\mu\text{-}Cl)_2Al^iBu_2]^+$ by reaction of $ClAl^iBu_2$ with the cation $[(SBI)Zr(\mu\text{-}H)_3(Al^iBu_2)_2]^+$ or with the dimeric dication $[((SBI)Zr)_2(\mu\text{-}Cl)_2]^{2+}$, both of which have been crystallographically characterized in the form of their $B(C_6F_5)_4^-$ salts (ref 13 and ref 18, respectively), has been described in ref 13. For the present study, we have prepared solutions of $[(SBI)Zr(\mu\text{-}Cl)_2AlMe_2]^+$ by reaction of $ClAlMe_2$ with the cation $[(SBI)Zr(\mu\text{-}Me)_2AlMe_2]^+$, in order to avoid the presence of potentially hydride-generating aluminum *iso*-butyl species (Supporting Information).

(18) Bryliakov, K. P.; Talsi, E. P.; Semikolenova, N. V.; Zakharov, V. A.; Brand, J.; Alonso-Moreno, C.; Bochmann, M. *J. Organomet. Chem.* **2007**, *692*, 859−868.

(19) The expected hyperfine splitting by the Zr-CH_3 group (∼5 G) remains unresolved under the line width (∼8 G) of the main signal in Figure 2.

(20) Attempts to reduce the cation $[(SBI)Zr(\mu\text{-}Me)_2AlMe_2]^+$ with cobaltocene likewise yielded substantial amounts of $(SBI)ZrMe_2$.

(21) Hyperfine splitting due to the minor isotope ^{91}Zr (I = 5/2, 11%) is not observed in this case, probably due to overlap with multiple splitting by ^{27}Al and ^1H nuclei.

(22) The EPR signal shown in Figure 3 is not compatible with a hyperfine splitting due to two ^{27}Al nuclei, e.g. in a complex $(SBI)Zr(\mu\text{-}H)_3(AlR_2)_2$.

(23) A similar EPR spectrum with hyperfine splitting by one Al nucleus, with $a(^{27}Al)$ = 5.9 G, and two hydrogen nuclei, with $a(^1H)$ = 3.1 G, in reaction media containing $(2\text{-Ph-ind})_2ZrCl_2$ and Al^iBu_3, had been assigned to a species $(2\text{-Ph-ind})_2Zr^{III}(\mu\text{-}Cl)(\mu\text{-}^i Bu)Al\ ^iBu_2$ by Lyakin et al. (ref 7). Such an assignment can be excluded in our case, due to the absence of Cl^- ions.

(24) For zirconocene hydride complexes with terminal Zr^{III}-H units, $a(^1H)$ values in the range of 6−7 G have been reported in ref 25a−d. Higher values of 7−9 G have been found for anionic hydride complexes (ref 26), while $a(^1H)$ values as low as 3−4 G have been observed for zirconocene phosphine hydride complexes (ref 27).

(25) (a) Samuel, E.; Maillard, P.; Gianotti, C. *J. Organomet. Chem.* **1977**, *142*, 289−298. (b) Hudson, A.; Lappert, M. F.; Pichon, R. *J. Chem. Soc., Chem. Commun.* **1983**, 374. (c) Bajgur, C. S.; Jones, S. B.; Petersen, J. L. *Organometallics* **1985**, *4*, 1929−1936. (d) Dioumaev, V. K.; Harrod, J. F. *Organometallics* **1997**, *16*, 1452−1464.

(26) Choukroun, R.; Gervais, D. *J. Chem. Soc., Chem. Commun.* **1985**, 224−225.

(27) Larsonneur, A.-M.; Choukroun, R.; Jaud, J. *Organometallics* **1993**, *12*, 3216−3224.

(28) Wehmschulte, R. J.; Power, P. P. *Polyhedron* **1999**, *18*, 1885−1888.

(29) Substantially diminished $a(^1H)$ values of 3 and 5 G (rather than $a(^1H)$ values of 7−10 G typical for titanocene complexes with terminal Ti^{III}−H units. Brintzinger, H. H. *J. Am. Chem. Soc.* **1967**, *89*, 6871−6876. Lukens, W. W.; Matsunaga, P. T.; Andersen, R. A. *Organometallics* **1998**, *17*, 5240−5247. They have also been observed in the dihydride-bridged titanocene complexes $(C_5H_5)_2Ti^{III}(\mu\text{-}H)_2AlCl_2$ and $(C_5H_5)_2Ti^{III}(\mu\text{-}H)_2AlH_2$, respectively. Henrici-Olive, G.; Olive, S. *J. Organomet. Chem.* **1970**, *23*, 155−157.

(30) Reduction of $(SBI)ZrMe_2$ to a Zr(III) species by reductive alkane elimination (eqs 4, 6) would produce only 1/2 equiv of R−H. Formation of close to 1 equiv of alkane (Supporting Information) indicates the simultaneous operation of some additional, as yet unidentified, reaction(s).

(31) (a) Lappert, M. F.; Pickett, C. J.; Riley, P. I.; Yarrow, P. I. *J. Chem. Soc., Dalton Trans.* **1981**, 805−813. (b) Lappert, M. F.; Raston, C. L.; Skelton, B. W.; White, A. H. *J. Chem. Soc., Dalton Trans.* **1997**, 2895−2902.

(32) An EPR doublet with $a(^{31}P)$ = 20.6 has been reported by Dioumaev and Harrod for the related complex $(C_5H_5)_2Zr(^n Bu)PMe_3$ (ref 25d).

(33) Herrmann, W. A.; Rohrmann, J.; Herdtweck, E.; Spaleck, W.; Winter, A. *Angew. Chem., Int. Ed. Engl.* **1989**, *28*, 1511−1512.

(34) Pool, J. A.; Chirik, P. J. *Can. J. Chem.* **2005**, *83*, 286−295.

(35) Hitchcock, P. B.; Lappert, M. F.; Lawless, G. A.; Olivier, H.; Ryan, E. J. *J. Chem. Soc., Chem Commun.* **1992**, 474−476.
(36) Gambarotta, S.; Chiang, M. Y. *Organometallics* **1987**, *6*, 897−899.
(37) Lauher, J. W.; Hoffmann, R. *J. Am. Chem. Soc.* **1976**, *98*, 1729−1742.
(38) McMahon, C. N; Francis, J. A.; Barron, A. R. *J. Chem. Crystallogr.* **1997**, *27*, 191−194.
(39) Lalama, M. S.; Kampf, J.; Dick, D. G; Oliver, J. P. *Organometallics* **1995**, *14*, 495−501.
(40) Asadi, A.; Avent, A. G.; Coles, M. P.; Eaborn, C.; Hitchcock, P. B.; Smith, J. D. *J. Organomet. Chem.* **2004**, *689*, 1238−1248.
(41) Chakraborty, D.; Chen, E. Y.-X. *Inorg. Chem. Commun.* **2002**, *5*, 698−701.
(42) Based on the stoichiometry described in eq. 4, there is not enough $HAl^{i}Bu_2$ to fully reduce **1**. Signals of **1** can thus still be observed by ^1H NMR even after long reaction times.
(43) The parent Zr(III) cation $[(C_5H_5)_2Zr^{III}]^+$ has been reported to give rise to a similarly narrow EPR signal at g = 1.996 with $a(^{91}Zr)$ = 12.3 G Dioumaev, V. K.; Harrod, J. F. *Organometallics* **1997**, *16*, 2798−2807.
(44) Urazowski, I. F.; Ponomaryev, V. I.; Nifant'ev, I. E.; Lemenovski, D. A. *J. Organomet. Chem.* **1989**, *368*, 287−294.
(45) Preliminary results indicate that $(SBI)Zr^{III}(\mu\text{-}Cl)_2AlMe_2$ is activated by methylalumoxane to polymerize propene at a rate about one-third of that with which propene is polymerized by $(SBI)ZrCl_2$ after activation with methylalumoxane under comparable conditions. Studies concerning the reactions leading to this activation are in progress in our laboratories.
(46) Stoll, S.; Schweiger, A. *J. Magn. Reson.* **2006**, *178*, 42−55.